X-RAY SCATTERING FROM LABELED MEMBRANES

J. STAMATOFF, T. BILASH, Y. CHING, AND P. EISENBERGER, *Bell Laboratories, Murray Hill, New Jersey 07974 U.S.A.*

ABSTRACT We present a new method for the determination of structural parameters in biological membranes. Recording the continuous scattering of heavy-atom labeled membranes and applying elementary Fourier methods we obtain the scattering of the heavy-atom distribution alone. The details of this distribution are explored by developing a simple model and testing for cases relevant to biological membranes. We find that the intensity distribution is highly sensitive to many key parameters. The increased signal from heavy-atom labeling and the use of an improved x-ray system make it possible to record patterns from dilute membrane suspensions. Thus determination of these parameters is possible in the same environment where many membrane biochemical studies are performed. Application of the method is made to a model lipid bilayer membrane, dipalmitoyl phosphatidylcholine by labeling with UO_2^{++} ions. We determine the precise distance between UO_2^{++} layers on either side of the membrane as well as the width of the label on each side. This determination permits estimation of phosphate separation across single labeled bilayers in an aqueous suspension.

INTRODUCTION

Small-angle x-ray diffraction from biological membranes has provided useful information. However, there are limitations and problems associated with the techniques. First, to improve the signal, membranes are stacked by ultracentrifugation and partial dehydration. Due to imperfections in the membrane stack, coherent diffraction decreases rapidly at large angles. Thus, the patterns are of limited resolution and Fourier reconstructions of projected electron densities are smeared making precise information (e.g., membrane width) difficult to determine. Second, biochemically distinguishable molecules (e.g., protein and lipids, or specific proteins) diffract x rays in the same manner determined by electron density. Thus projected electron density distributions are often ambiguous.

We present a method in this paper that minimizes the above problems. We study the scattering of heavy-atom labeled membranes with the use of an improved x-ray system. The increased scattering due to heavy atoms permits our x-ray system to record patterns from suspensions of single membranes. Analysis of the continuous scattering makes possible determination of the label's distribution. As a result, precise information (e.g., the membrane width) may be obtained without recording patterns to high resolution. This is possible for the same reason that lattice constants may be determined accurately from one diffraction order. Finally, through the use of specific labels, the method can provide information about specific membrane components. Thus some of the difficulties associated with complex projected electron density distributions may be avoided.

In this study we use dipalmitoyl lecithin as a model membrane. We bind UO_2^{++} ions to the bilayer in the same manner as Furuya et al. (1), thus obtaining a suspension of labeled single bilayers. While an exact comparison is difficult, our suspensions are 1–2 orders more dilute than those of Furuya and more comparable to concentrations expected for natural membrane

vesicles. By analyzing changes in the pattern as a function of the amount of UO_2^{++} we are able to determine the label distribution. We develop a model for label distributions and explore cases relevant to membranes.

MATERIALS AND METHODS

Dipalmitoyl phosphatidylcholine (DPPC) was purchased from Sigma Chemical Co., St. Louis, Mo. and used without further purification. Suspensions of DPPC were labeled with UO_2^{++} by the method of Furuya et al. (1) in distilled water. The molar ratios of UO_2^{++} to DPPC were 1:1, 1:2, 1:4, and 1:20. The samples contained <43 mg DPPC/ml of suspension.

Samples were x rayed at room temperature using the following apparatus. X rays from a bright rotating copper anode source (70 KW/mm^2) are point focused to a (0.5 mm)^2 spot using a large doubly curved quartz crystal (75 × 25 mm) (2). The scattered x rays are detected using a stable position sensitive x-ray detector with a nichrome wire anode filled with Ar-CH_4 at 100 pounds/in^2. The detector is ≈90% efficient. Charge division position encoding is used. The net enhancement factor is between 100 and 1,000 compared to conventional schemes using film and mirror-monochromator focusing devices.

RESULTS

Figs. 1–4 show the scattering of UO_2^{++} labeled bilayers for each of the four molar ratios. These are plotted as a function of $S = 2 \sin \theta/\lambda$, where 2θ is the scattering angle. For these patterns, camera background is removed in the following manner. In place of a beam stop, 0.010 inch of brass is used to attenuate the central beam. Background, recorded without a sample, is scaled to the same integrated beam value as that of the pattern and then subtracted. Background due to the scattering of water is removed by scaling patterns from water plus sample and water together at large angles after correcting each pattern for camera background and then subtracting. The background-removed patterns are finally corrected for

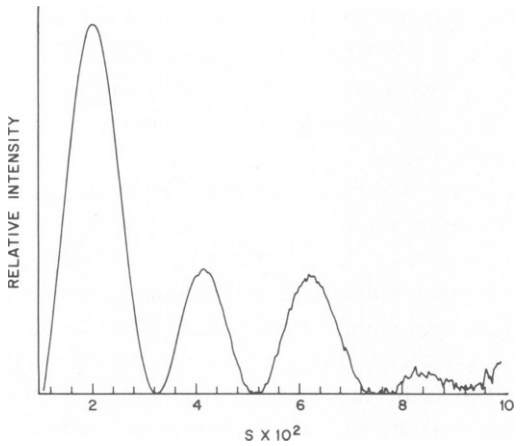

FIGURE 1

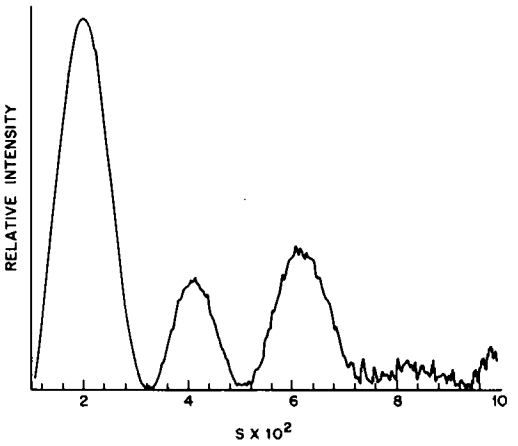

FIGURE 2

FIGURE 1 The pattern of a 1:1, UO_2^{++}:DPPC suspension. The intensity is corrected for background and spherical averaging. $S = 2\sin\theta/\lambda$ and is in units of Å^{-1}. The suspension is in distilled water and contains 38.5 mg DPPC/ml.

FIGURE 2 The patterns of 1:2, UO_2^{++}:DPPC suspension. The intensity is corrected for background and spherical averaging. S is the same as in Fig. 1. The suspension contains 38.7 mg DPPC/ml.

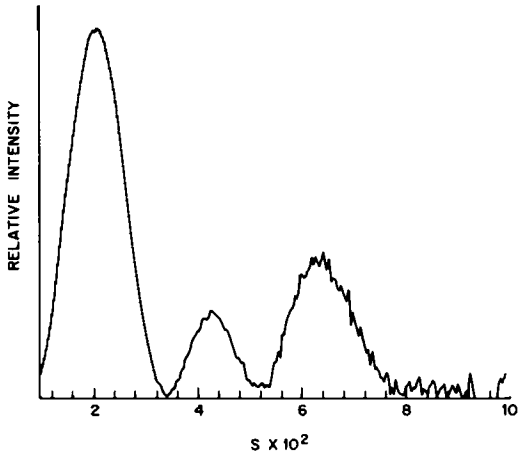

FIGURE 3

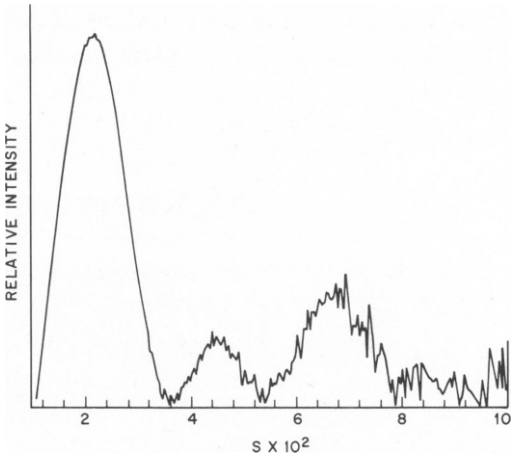

FIGURE 4

FIGURE 3 The pattern of a 1:4, UO_2^{++}:DPPC suspension. The intensity is corrected for background and spherical averaging. S is the same as in Fig. 1. The suspension contains 42.2 mg DPPC/ml.
FIGURE 4 The pattern of a 1:20, UO_2^{++}:DPPC suspension. The intensity has been corrected for background and spherical averaging. S is the same as in Fig. 1. The suspension contains 29.3 mg DPPC/ml. This is essentially the pattern of pure DPPC. UO_2^{++} ions have been added to prevent multilayering.

spherical averaging by a Lorentz factor of S^2 (3). After this processing we find that the minima are not precisely zero due to in-plane scattering. For the 1:1, UO_2^{++}:DPPC ratio this in-plane diffraction has been previously noted (1). To obtain the scattering from electron density variations through the plane of the bilayer, we further subtract a straight line background passing through the minima shown in Figs. 1–4.

The pattern for the 1:1, UO_2^{++}:DPPC ratio agrees with that previously published by Furuya et al. Progressive changes take place as amount of UO_2^{++} is decreased. The second lobe of intensity decreases with respect to the others. In addition, the position of the maximum and minimum shift.

THEORY

We assume that the UO_2^{++} ions are distributed on both sides of the bilayer and randomly distributed within the plane of the bilayer. The bilayers can be considered to form either vesicles of varying diameters or widely separated randomly oriented flat sheets. For vesicles of varying diameters, Lesslauer et al. (4) have shown that the scattering is equivalent to that of randomly oriented flat sheets. This scattering is, in general, due to electron density variations both within and through the plane of the bilayer. However, within the plane, lipid bilayers are essentially without structure on the distance scale of our scattering experiments. Thus the bilayer scattering is accurately described by electron variations through the bilayer (i.e., the scattering is due to changes in the electron density projected on an axis orthogonal to the bilayer surface).

For heavy-atom labeled bilayers, the scattering is from both heavy atoms and the bilayer.

For the present, neglecting the bilayer, the general expression for the scattered intensity of two heavy-atom layers separated by a distance d is:

$$I = f^2 \sum_{ij} \cos(2\pi \boldsymbol{S} \cdot \boldsymbol{r}_{ij})$$

$$= f^2 \sum_{ij} [\cos(2\pi \boldsymbol{S}_\perp \cdot \boldsymbol{r}_{ij})\cos(2\pi \boldsymbol{S}_\parallel \cdot \boldsymbol{r}_{ij}) - \sin(2\pi \boldsymbol{S}_\perp \cdot \boldsymbol{r}_{ij})\sin(2\pi \boldsymbol{S}_\parallel \cdot \boldsymbol{r}_{ij})],$$

where $\boldsymbol{r}_{ij}$ are the heavy-atom interatomic vectors and f is the atomic scattering factor. $\boldsymbol{S}_\perp$ and $\boldsymbol{S}_\parallel$ are components of $\boldsymbol{S}$ which are orthogonal and parallel to the bilayer plane. For randomly distributed atoms, for every $\boldsymbol{r}_{ij}$ there is a $\boldsymbol{r}_{lm}$ such that:

$$\boldsymbol{S}_\parallel \cdot \boldsymbol{r}_{ij} \simeq -\boldsymbol{S}_\parallel \cdot \boldsymbol{r}_{lm}$$

and

$$\boldsymbol{S}_\perp \cdot \boldsymbol{r}_{ij} \simeq \boldsymbol{S}_\perp \cdot \boldsymbol{r}_{lm}.$$

This is true for pairs on one side of the bilayer (for which $\boldsymbol{S}_\perp \cdot \boldsymbol{r}_{ij} = 0$) and for pairs across the bilayer. Therefore,

$$I \simeq f^2 \sum_{ij} \cos(2\pi \boldsymbol{S}_\perp \cdot \boldsymbol{r}_{ij})\cos(2\pi \boldsymbol{S}_\parallel \cdot \boldsymbol{r}_{ij}).$$

Thus even with the approximate symmetry condition imposed, the expression for intensity contains terms responsive to the in-plane distribution. For a large number of randomly distributed heavy atoms, the intensity may also be expressed as:

$$I \simeq 2f^2(1 + \cos(2\pi |\boldsymbol{S}_\perp| d) \sum_{ij} \cos(2\pi \boldsymbol{S}_\parallel \cdot \boldsymbol{r}_{ij}),$$

where $1 + \cos(2\pi |\boldsymbol{S}_\perp| d)$ shows the contribution of pairs on one side or across the bilayer, and the sum now extends over pairs on one side.

We can now explore the intensity function. For $\boldsymbol{S}_\parallel = 0$,

$$I \simeq f \frac{N^2}{2} (1 + \cos(2\pi |\boldsymbol{S}_\perp| d))$$

or

$$I \simeq f^2 N^2 \cos^2(\pi |\boldsymbol{S}_\perp| d),$$

where N is the total number of heavy atoms. For $\boldsymbol{S}_\parallel \neq 0$,

$$I \simeq 2f^2(1 + \cos(2\pi |\boldsymbol{S}_\perp| d)\left(\sum_{\substack{ij \\ i \neq j}} \cos(2\pi \boldsymbol{S}_\perp \cdot \boldsymbol{r}_{ij}) + \sum_{i=1}^{N/2} 1\right).$$

Thus we have,

$$I \simeq 2Nf^2 \cos^2(\pi |\boldsymbol{S}_\perp| d).$$

For large N, the scattering is therefore concentrated on an axis perpendicular to the bilayer

plane. Random orientation of the sheets spherically averages the intensity in a manner approximated by division by S^2. Having reduced the problem to one dimension, the detailed modeling is best performed using analytic functions and Fourier integral methods.

Consider a membrane of average width d. Let there be α units of label distributed according to a Gaussian function of width W_α on one side of the membrane. On the other side let there be $N - \alpha$ units of label distributed according to a Gaussian function of width W_N. N, the total amount of label will remain constant (Fig. 5). For this case, the Fourier transform is:

$$F(S) = (N - \alpha)G_N e^{i\pi sd} + \alpha G_\alpha e^{-i\pi sd},$$

where

$$G_{N/\alpha} = e^{-\pi W_{N/\alpha}^2 s^2}$$

is the transform of the Gaussian

$$\frac{1}{W_{N/\alpha}} e^{-\pi Z^2/W_{N/\alpha}^2},$$

so that the intensity $I(s)$ is given by:

$$I(S) = F^*F(s) = (NG_N - (G_N + G_\alpha)\alpha)^2 + 4\alpha(N - \alpha)G_N G_\alpha \cos^2 \pi sd.$$

We have the following special cases: (a) $W_N = W_\alpha$; equal widths on both sides of the membrane: $I(s) = G_N^2[(N - 2\alpha)^2 + 4\alpha(N - \alpha)\cos^2 \pi sd]$. ($b$) $\alpha = N/2$ and $W_N = W_\alpha$; the symmetric case: $I(s) = N^2 G_N^2 \cos^2 \pi sd$. ($c$) $\alpha = 0$; totally asymmetric case: $I(s) = N^2 G_N^2$. In

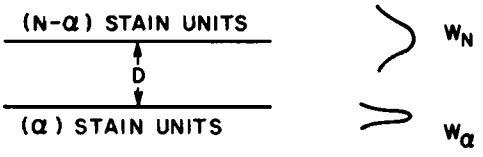

FIGURE 5

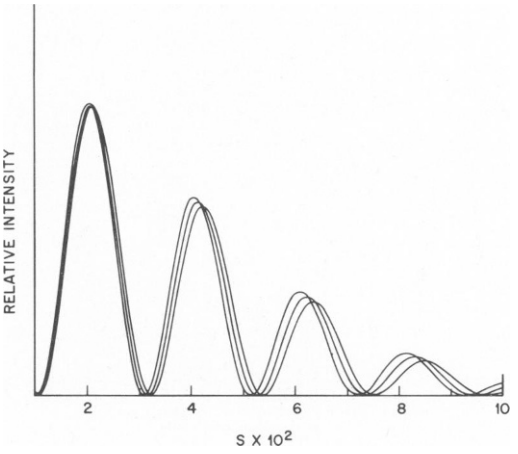

FIGURE 6

FIGURE 5 Schematic of the model analyzed (see Theory). There are $N - \alpha$ units of label distributed on one side according to a Gaussian of width W_N. On the other side, separated by a distance d, there are α units distributed with width W_N.

FIGURE 6 Intensity for the model as a function of d. $N = 2$, $\alpha = N/2$ (symmetric case), $W_N = W_\alpha$, $W_{1/2} = 7.5$ Å, and $d = 46.5$, 47.5, or 48.5 Å. The highest frequency ripple corresponds to the largest value of d.

Figs. 6–8, we show the effects of changing various parameters. In all of these calculations $W_N = W_\alpha$ and $N = 2$. Fig. 6 shows the effect of varying d in 1-Å increments with $W_{1/2} = 7.5$ Å and $\alpha = N/2$ (symmetric case). Here $W_{1/2}$ is the full width at half maximum of the Gaussian and equals:

$$2\sqrt{\frac{\ell n 2}{\pi}}\, W_N.$$

Fig. 7 shows the consequences of varying $W_{1/2}$ by 2.5-Å increments with $d = 47.5$ Å and $\alpha = N/2$. Fig. 8 shows the effect of varying α with $W_{1/2} = 7.5$ Å and $d = 47.5$ Å. Comparing with our data, we estimate sensitivities of ≈ 1 Å for d, ≈ 2 Å for $W_{1/2}$, and ≈ 0.1 for α.

For an actual membrane, we are concerned with the projection of the heavy atom distribution on an axis orthogonal to the membrane plane. We assume that for most membranes variations of the label distribution parallel to the membrane surface will be relatively small and disordered, thus (as previously shown) contributing little in the angular region we are sampling. The function G_N/α is therefore a monitor of surface roughness of the membrane (or more precisely, the projection of a rough label distribution on an axis orthogonal to the membrane plane). In the analysis, $G_{N/\alpha}$ is taken to be Gaussian. In general, by performing experiments in which either side of the membrane is labeled G_N, G_α, N, and α may be determined.

For DPPC, the observed patterns do not resemble any of these calculations. One reason is that the contribution of the bilayer to the scattering has been neglected in the model. The scattering due to the label alone may be obtained by considering this contribution in the following manner. First, following the "heavy-atom" assumption used by Furuya et al., the

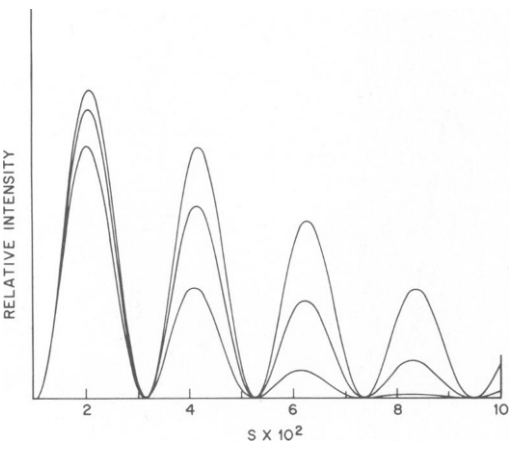

FIGURE 7

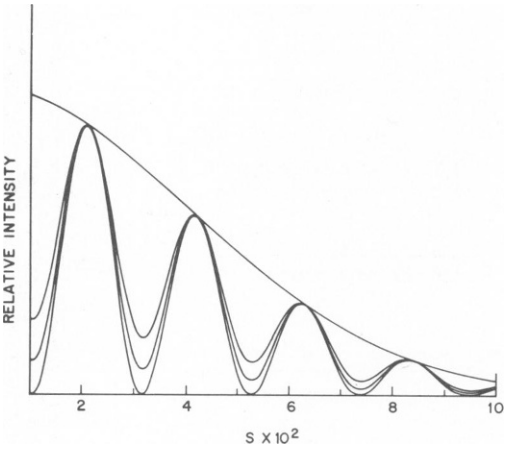

FIGURE 8

FIGURE 7 Intensity for the model as a function of $W_{1/2}$. $N = 2$, $\alpha = N/2$ (symmetric case), $d = 47.5$ Å, and $W_{1/2} = 10.0$, 7.5, and 5.0 Å. The most rapidly damped ripple corresponds to the largest value of $W_{1/2}$.
FIGURE 8 Intensity for the model as a function of α. $N = 2$, $d = 47.5$ Å, $W_{1/2} = 7.5$ Å, and $\alpha = 1.0$, 0.666, 0.5, and 0.0. For these cases, the ratio of the amount of the label on one side to that on the other side is $(N - \alpha)/\alpha = 1, 2, 3$, and ∞. The minima become progressively more shallow as the degree of asymmetry increases.

Fourier transform may be obtained from the intensity distribution by taking the square root and assigning alternate signs to the first three lobes. The transform for higher concentrations of label may be obtained from the lower concentration by adding the parameterized function for the label as follows:

$$[K_H e^{(-\pi W^2 s^2)} \cos(\pi s d) + K F_{1:20}(s)] = F(s),$$

where K_H and K are scaling constants and $F(s)$ is the transform to be calculated [which may be $F_{1:4}(s)$,$F_{1:2}(s)$, or $F_{1:1}(s)$]. The values of the parameters determined by a nonlinear least-squares routine are given in Table I. The calculations were performed over the range $0.014 \leq S \leq 0.07$. Fig. 9 shows the calculated vs. actual intensities for the 1:1, UO_2^{++}:DPPC ratio.

DISCUSSION

The basis for our analysis is the assumption that the label varies isomorphously. Proceeding to fit higher UO_2^{++}:DPPC ratio data with the sum of the 1:20 ratio data and a parameterized function for the heavy-atom scattering, we accomplish two things. First, we determine parameter values that accurately model the heavy-atom scattering. Second, we verify (by virtue of the accuracy of the fit) that the isomorphous assumption is correct. Thus, the parameters W and d are, to within their respective uncertainties, identical for each heavy-atom ratio analyzed.

This determination should be more precise than direct Fourier inversion, which suffers from lack of resolution. In this specific application to DPPC, there is larger uncertainty in the Gaussian width, W, than in the layer separation, d. This is due to significant correlation between W and the scaling parameter, K_H. Smaller uncertainty (for less correlation between

TABLE I

$F(s) = K_H e^{-\pi W^2 s^2} \cos \pi s d + K F_{1:20}(s)$

$F(s)$	K	K_H	W	d	er*
UO_2:DPPC			Å	Å	%
1:1	0.834	78.332	6.2 ± 2	49.6 ± 1.2	0.324
1:2	0.451	27.038	3.1	51.0 ± 1.8	0.796
			0→7		
1:4	0.559	15.787	0.0	50.2 ± 2.6	0.949
			0→8		

The fit was accomplished by comparing the 1:20, UO_2^{++}:DPPC data with each of the higher concentrations using the summation given in the title above. Uncertainties for W and d are also given. Since W must be >0, but enters the equation as the square, the uncertainty is given with a minimum of 0 (e.g., 0→7).

*The percent error is calculated as follows:

$$er = \frac{\sum_i (F(s_i) - F(s_i)_{\text{calculated}})^2}{\sum_i F(s_i)^2} \times 100,$$

where the sums are over the observed data points.

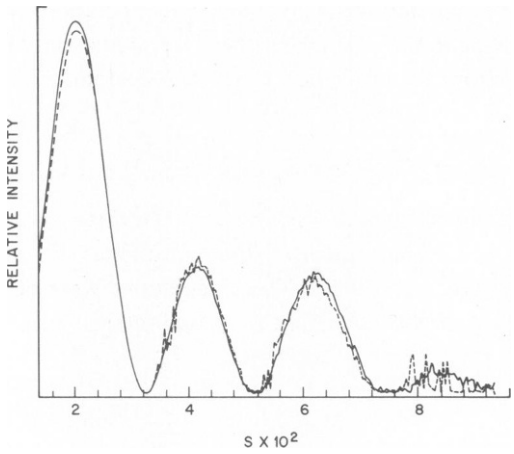

FIGURE 9 The intensity calculated from the 1:20, UO_2^{++}:DPPC ratio by the addition of a label scattering function (dashed line) vs. the observed intensity for the 1:1 ratio (solid line). The parameters for the function are given in Table I.

W and K_H) would also result if W were larger. The parameter d is more accurately determined and is essentially uncorrelated with the other parameters.

We note (in agreement with Furuya et al.) that the maxima and zeros shift significantly upon varying the UO_2^{++}:DPPC ratio. For $I_{1:20}$, the maxima for the first three lobes occur at ≈46.5, 22.1, and 14.8 Å. For $I_{1:1}$, the maxima are ≈48.8, 24.0, and 16.1 Å. Thus the maxima correspond to a larger distance for $I_{1:1}$.

Based on our analysis, the progressive increase in the spacing for the first lobe maximum is comprehensible. We have determined the periodicity of the heavy-atom scattering curve to be 50.3 Å. Isomorphously adding more heavy atoms produces this shift in the scattering curve toward the maximum for heavy atoms only. This shift does not imply that the lecithin bilayer is changing. Our analysis suggests, in fact, that the bilayer is constant. Thus, at any particular heavy-atom concentration, the spacing of the first lobe maximum has only an approximate meaning in terms of membrane width. The periodicity of the $I_{1:20}$ pattern compared with the 50.3-Å periodicity of the label scattering function shows the magnitude of the approximation employed when membrane widths are calculated from the intensity maxima of unlabeled membranes (3). This is of particular concern for concentrated membrane dispersions for which the lipid profile may not dominate and which may have, in addition, some intermembrane interference effects.

Provided that the label contributes significantly to the scattering, the heavy-atom assignment of phase angles should prove correct. The method is exactly analogous to that widely used in crystallography. For the case of DPPC, the assignment of different signs would lead to sharp changes in the Fourier transform. The smooth sinusoidal nature of the transform, for the signs chosen, suggest that the assignment is correct. For isomorphously incorporated label, the heavy-atom assumption is not required. Here:

$$(F_M(s) + \alpha F_H(s))^2 = I_M + \alpha F_M F_H + I_H = I_\alpha(s),$$

where $F_M(s)$ is the transform of the membrane, $I_M = F_M^* F_M(s)$; $F_H(s)$ is the transform of the

heavy-atom distribution, $I_H = F_H^* F_H(s)$; and $I_\alpha(s)$ is the observed intensity at label concentration α.

For three different concentrations α, the cross term $F_M F_H$ and I_M may be eliminated to obtain I_H. Therefore the label's intensity curve may be obtained for complex asymmetric membranes without phase-angle information. This is particularly important since phase angles are not restricted to 0 or π radians for single asymmetric membranes.

The enhancement of net scattering due to the label is significant. We have found that the signal to background increases by ≈ 5 in the first lobe for 1:1 vs. 1:20, UO_2^{++}:DPPC. This enhancement has made possible recording similar patterns for erythrocyte membrane suspensions.[1] Thus extreme preparative conditions may be avoided.

An obvious extension of this method would be to use specific heavy-atom labels. Such labeling has been accomplished for bacteriorhodopsin (5). For these cases, specific information about particular proteins may be obtained.

In this study, we find that the bilayer is 50.3 Å thick in an aqueous environment. More precisely, the separation between UO_2^{++} layers is 50.3 Å (an average of the three determinations). Shah (6) and Chapman et al. (7) show that UO_2^{++} ions bind to the phosphate moiety in DPPC. Based on these studies, we conclude that the UO_2^{++}-phosphate complex maintains this separation in an aqueous environment. Direct interpretation in terms of phosphate separation for unstained isolated bilayers is not possible due to our inability to rule out changes in the bilayer imparted by UO_2^{++} binding. However, our isomorphous results show that such alterations must take place at UO_2^{++}:DPPC ratios of less than 1:20.

We believe that this method should find wide application in membrane systems. The precise information available permits one to pose detailed questions that were previously unanswerable. This has been demonstrated in our first application to DPPC. The ability to ask such questions in the same suspension state where membrane biochemistry is performed makes this approach quite appealing. The potential use of specific labels is of obvious value.

We thank Dr. B. Kincaid for his valuable suggestions.

Received for publication 26 July 1978 and in revised form 13 August 1979.

REFERENCES

1. FURUYA, K., T. YAMAGUCHI, Y. INOKO, and T. MITSUI. 1976. Structures of uranyl-decorated lecithin and lecithin-cholesterol bilayers. *Acta. Cryst.* **B32**:1811.
2. BERREMAN, D., J. STAMATOFF, and S. J. KENNEDY. 1977. Doubly curved crystal point-focussing x-ray monochromators: geometrical and practical optics. *Appl. Opt.* **16**:2081.
3. WILKINS, M. H. F., A. E. BLAUROCK, and D. M. ENGELMAN. 1971. Bilayer structure in membranes. *Nat. New Biol.* **230**:72.
4. LESSLAUER, W., J. CAIN, and J. K. BLASIE. 1971. On the location of 1-anilino-8-naphthalene-sulfonate in lipid model systems. *Biochim. Biophys. Acta.* **241**:547.
5. DUMONT, M., and J. W. WIGGINS. 1978. Platinum labeling of bacteriorhodopsin. *Biophys. J.* **21**:74*a*.
6. SHAH, D. 1969. Interaction of uranyl ions with phospholipid and cholesterol monolayers. *J. Colloid Interface Sci.* **29**:210.
7. CHAPMAN, D., J. URBINA, and K. M. KEOUGH. 1974. Biomembrane phase transitions. *J. Biol. Chem.* **249**:2512.

[1]Stamatoff, J., T. Bilash, and Y. Ching. X-ray scattering studies of heavy-atom bound erythrocyte membrane suspensions. Submitted for publication.